HIGHLIGHTS FROM THE NA61/SHINE EXPERIMENT AT THE CERN SPS*

Marta Urbaniak †, Szymon Puławski, Seweryn Kowalski
for the NA61/SHINE Collaboration

Institute of Physics, University of Silesia, Katowice, Poland

Received 29 December 2025, accepted 1 February 2026, published online 22 April 2026

The NA61/SHINE strong interaction program is dedicated to exploring the properties of strongly interacting matter under extreme conditions. Its central objectives are the search for the critical point in the QCD phase diagram and the study of the properties of the onset of deconfinement. This contribution summarizes selected recent achievements of the NA61/SHINE Collaboration, including results on hadron production, fluctuations, and correlations, and outlines future prospects for the experiment.

DOI:10.5506/APhysPolBSupp.19.2-A12

1. Introduction

NA61/SHINE is a multipurpose fixed-target experiment operating at the CERN Super Proton Synchrotron (SPS) [1]. Its experimental program covers strong interaction, neutrino, and cosmic-ray physics. In the neutrino program, NA61/SHINE provides precise hadron production measurements for experiments at J-PARC and Fermilab, while the cosmic-ray program delivers data essential for the interpretation of extensive air showers, supporting projects such as the Pierre Auger Observatory, KASCADE, and satellite-based experiments. The strong interaction program focuses on a systematic study of strongly interacting matter under extreme conditions, including investigations of the onset of deconfinement in light- and intermediate-mass systems, searches for the critical point of the QCD phase diagram, and studies of open charm production in heavy-ion collisions. The program is based on systematic beam momentum scans with collision systems ranging from p+p to Pb+Pb, using ion beams (Be, Ar, Xe, Pb) with momenta $p_{\text{beam}} = 13\,A$–$150\,A\,\text{GeV}/c$ and hadron beams (π, K, p) with momenta $p_{\text{beam}} = 13$–400 GeV/c, corresponding to center-of-mass energies per nucleon pair of $\sqrt{s_{NN}} = 5.1$–16.8 (27.4) GeV.

* Presented at the XLVI International Conference of Theoretical Physics "Matter to the Deepest", Katowice, Poland, 15–19 September, 2025.

† Corresponding author: marta.urbaniak@us.edu.pl

2. Properties of the onset of deconfinement

The characteristic structures that signal the creation of the quark–gluon plasma are known as the kink, horn, and step [2]. They are obtained through the analysis of particle spectra and yields. The NA49 experiment observed a pronounced peak (horn) in the K^+/π^+ ratio, which was interpreted as an indication of the onset of deconfinement [3]. The NA61/SHINE experiment investigates whether these characteristic structures — the kink, horn, and step — also appear in collisions involving light- and intermediate-mass nuclei.

The step plot shown in Fig. 1 represents the inverse slope parameter of the transverse mass/transverse momentum spectra of K^+ and K^-. The parameter T reflects the thermal freeze-out temperature and the radial flow velocity. A similar energy dependence is observed for p+p, Be+Be, Ar+Sc, and Pb+Pb collisions. A clear step-like structure in T is visible across all

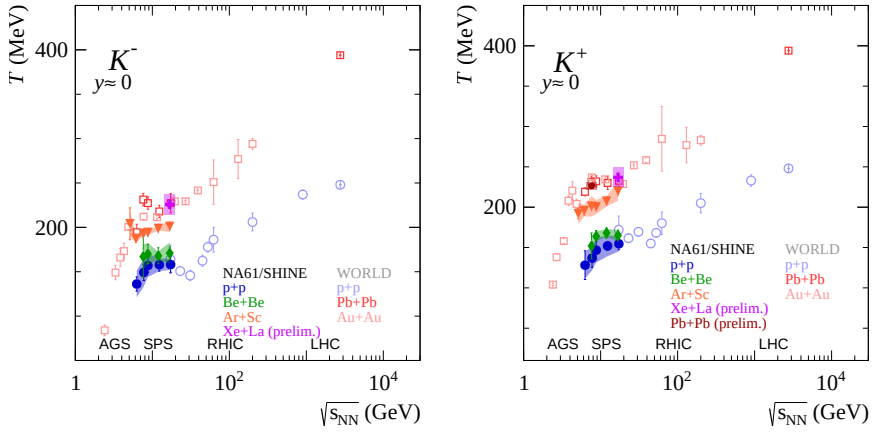

Fig. 1. Step plots — inverse slope parameter of transverse mass/transverse momentum spectra of K^+ (right plot) and K^- (left plot). For the references, see NA61/SHINE measurements: Ar+Sc [8], Be+Be [9], and p+p [10]; for world data, see Ref. [8]. For preliminary Xe+La and Pb+Pb data, the following center-of-mass rapidity ranges were used: $0.4 < y < 0.6$ for Xe+La and $0.8 < y < 1.0$ for Pb+Pb.

systems, with the magnitude of T increasing with the system size. The horn plot is shown in Fig. 2. The ratio K^+/π^+ is approximately proportional to the strangeness-to-entropy ratio, which differs between the confined hadronic phase and the quark–gluon plasma (QGP). For both the step and horn structures, the p+p results are close to those for Be+Be, while Xe+La approach to those for Pb+Pb. For Ar+Sc, a horn structure was not observed. The new NA61/SHINE Pb+Pb data at $\sqrt{s_{NN}} = 7.6$ GeV confirm the earlier NA49 observations for the inverse slope parameter T and the K^+/π^+ ratio.

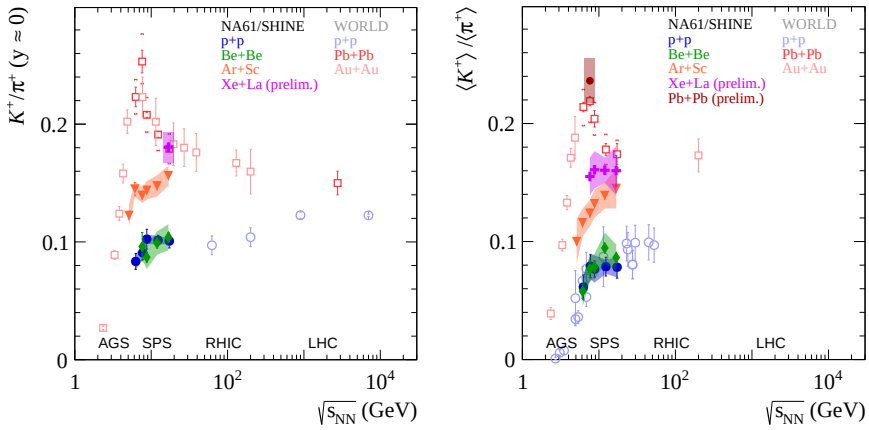

Fig. 2. Horn plots — K^+/π^+ ratio *versus* energy at mid-rapidity (left plot) and in 4π (right plot). For the references, see NA61/SHINE measurements: Ar+Sc [8], Be+Be [9], and p+p [10]; for world data, see Ref. [8]. The NA61/SHINE Xe+La and Pb+Pb data are preliminary. The K^+/π^+ ($y \approx 0$) ratio in Xe+La was obtained in the rapidity interval $0.4 < y < 0.6$.

Figure 3 presents the K^+/π^+ ratio (left) and the inverse slope parameter of the K^+ transverse mass/transverse momentum spectra (right) as functions of the system size. The data indicate an increase in both the K^+/π^+ ratio and T with the system size. As mentioned earlier, the p+p results are

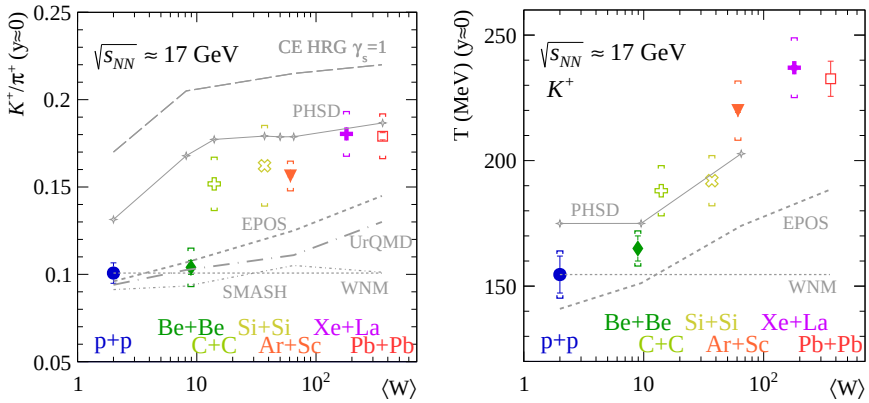

Fig. 3. The K^+/π^+ ratio (left) and the inverse slope parameter T of the K^+ transverse mass/transverse momentum spectra (right) as functions of the system size. For the references, see NA61/SHINE measurements: Ar+Sc [8], Be+Be [9], and p+p [10]; for world data (C+C, Si+Si, Pb+Pb), see Ref. [8]. Preliminary NA61/SHINE Xe+La data were obtained in $0.4 < y < 0.6$. The data are compared with predictions of EPOS [4], SMASH [5], PHSD [6], UrQMD, and HRG [7].

similar to those obtained for Be+Be, while the Xe+La results tend to approach those for Pb+Pb. The data are compared with predictions from the EPOS [4], SMASH [5], PHSD [6], UrQMD (and HRG) [7] models, none of which reproduces the full trend of the experimental results across the entire mean wounded-nucleon $\langle W \rangle$ range.

2.1. Search for the critical point

If the system freezes out near the critical point, its properties are expected to differ from those of an ideal gas. Fluctuations and correlations are therefore studied as key observables in the search for the critical point of strongly interacting matter, since enhanced fluctuations are expected in its vicinity, in analogy to critical opalescence observed near the liquid–gas phase transition [11]. Within the NA61/SHINE experiment, the intermittency of protons has been studied in Ar+Sc interactions at $\sqrt{s_{NN}} = 5.1$–16.8 GeV [12] and in Pb+Pb collisions at $\sqrt{s_{NN}} = 5.1$ and 7.6 GeV [13], as well as the intermittency of negatively charged hadrons in Xe+La interactions at $\sqrt{s_{NN}} = 16.8$ GeV [14]. No signal indicating the presence of a critical point was observed, suggesting that within the explored phase diagram region, the fluctuations remain consistent with non-critical behavior. In the NA61/SHINE intermittency analysis, statistically independent data points and cumulative variables are used [15, 16].

Another important line of studies in the search for the critical point is femtoscopy. A femtoscopy analysis was conducted for identical (like-sign) charged pions, modeling the particle-emitting source with a Lévy-type distribution. The two-particle Bose–Einstein correlation function was described by the equation

$$C_2(q) = 1 + \lambda \, \mathrm{e}^{-|qR|^{\alpha}} , \tag{1}$$

where q is the relative momentum between the pion pair, λ quantifies the correlation strength, R indicates the characteristic homogeneity length of the system, and α defines the shape of the emission profile. Specifically, $\alpha = 2$ corresponds to a Gaussian source, $\alpha = 1$ represents a Cauchy-like distribution, and smaller values of α (typically $\lesssim 0.5$) could signal proximity to the QCD critical point [17].

The results of the comprehensive energy scan using 0–10% central Ar+Sc collisions, together with point from Be+Be, are presented in Fig. 4, where the Lévy index α is shown as a function of the collision energy. For Be+Be collisions, the Lévy exponent α is far from the Gaussian value ($\alpha = 2$) and remains close to a Cauchy distribution ($\alpha = 1$). In Ar+Sc collisions, the α values are far from Cauchy, starting near the Gaussian limit and decreasing toward intermediate SPS energies. A constant fit to the transverse mass

(m_{T}) dependence of α values suggests a subtle minimum at mid-range SPS energies. Nevertheless, no indication of the critical point is observed, as the measured α values remain far from the predictions for critical behavior.

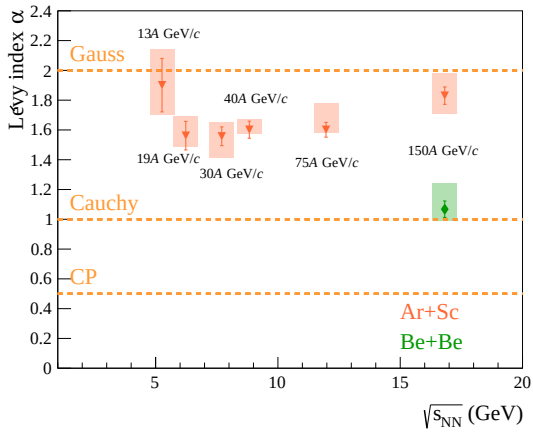

Fig. 4. The Lévy index α as a function of collision energy for 0–20% central Be+Be [18] with later estimate of systematic uncertainty and 0–10% central Ar+Sc (NA61/SHINE preliminary) interactions. Vertical bars represent statistical uncertainties, and colored boxes indicate systematic ones.

2.2. Anomaly in charged/neutral kaon production

The NA61/SHINE experiment recently presented possible evidence of isospin symmetry violation in high-energy Ar+Sc collisions at $\sqrt{s_{NN}} = 11.9$ GeV [19]. If isospin symmetry holds exactly, collisions between nuclei with $N = Z$ (isospin-symmetric nuclei) should produce equal numbers of isospin-symmetric particles, so the kaon multiplicities should follow the relations $\langle K^+\rangle(u\bar{s}) = \langle K^0\rangle(d\bar{s})$, $\langle K^-\rangle(\bar{u}s) = \langle \bar{K}^0\rangle(\bar{d}s)$. Consequently, the ratio

$$R_K \equiv \frac{\langle K^+\rangle + \langle K^-\rangle}{\langle K^0\rangle + \langle \bar{K}^0\rangle} = \frac{\langle K^+\rangle + \langle K^-\rangle}{2\langle K^0_{\mathrm{S}}\rangle} \tag{2}$$

is expected to be unity. The right-hand side of the equation relies on the fact that, neglecting the small effects of charge-parity violation, the multiplicities corresponding to the weak eigenstates can be expressed as $\langle K^0_{\mathrm{S}}\rangle = \frac{1}{2}\langle K^0\rangle + \frac{1}{2}\langle \bar{K}^0\rangle = \langle K^0_{\mathrm{L}}\rangle$.

Rapidity distributions ($\mathrm{d}N/\mathrm{d}y$) of K^0_{S} mesons (blue points) and the average of charged kaons $(K^+ + K^-)/2$ (green points) produced in central (0–10%) Ar+Sc collisions at $\sqrt{s_{NN}} = 11.9$ GeV can be seen in Fig. 5 (left plot). The transverse momentum (p_{T}) distributions for the same collision

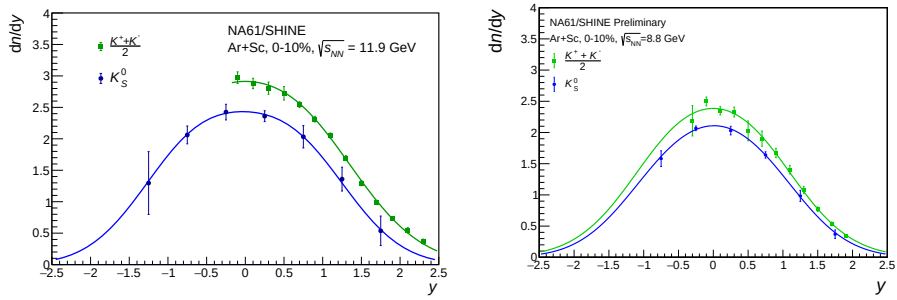

Fig. 5. Rapidity distributions ($\mathrm{d}N/\mathrm{d}y$) of K^0_S mesons (blue points) and the average of charged kaons $(K^+ + K^-)/2$ (green points) produced in central (0–10%) Ar+Sc collisions at $\sqrt{s_{NN}} = 11.9$ GeV (left) [19] and preliminary results at $\sqrt{s_{NN}} = 8.8$ GeV (right). The vertical bars represent the total uncertainties.

system, energy, and centrality class are shown in Fig. 6. Measurements indicated that charged kaons are emitted significantly more often than neutral kaons — by $(18.4 \pm 6.1)\%$ in the mid-rapidity range. The significance of the isospin violation is 4.7σ. The reported 4.7σ significance is not based solely on the NA61/SHINE data but also includes additional data points shown in Fig. 7, excluding the result at $40A\,\mathrm{GeV}/c$. An excess of charged over neutral K meson production, at the level of about 12%, was also observed in central Ar+Sc collisions at $\sqrt{s_{NN}} = 8.8$ GeV; rapidity distributions ($\mathrm{d}N/\mathrm{d}y$) can be seen in Fig. 5 (right plot).

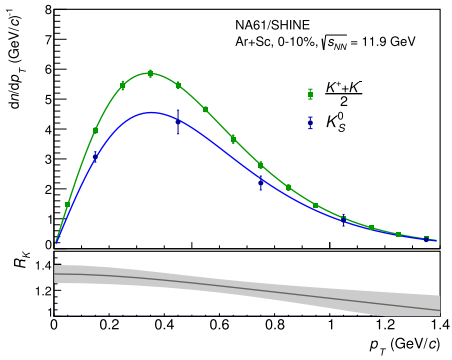

Fig. 6. Transverse momentum (p_T) distributions of K^0_S mesons (blue points) and the average of charged kaons $(K^+ + K^-)/2$ (green points) produced in central (0–10%) Ar+Sc collisions at $\sqrt{s_{NN}} = 11.9$ GeV [19]. The bottom panel of the figure presents the ratio of the two fitted curves, with its uncertainty band obtained by the propagation of the uncertainties of the fitted parameters. The vertical bars represent the total uncertainties.

Theoretical models of particle production that account for all known effects of isospin symmetry breaking do not adequately explain the magnitude of the observed effect. Precise measurements and theoretical modeling are still required for a systematic understanding of the observed isospin symmetry violation. Figure 7 shows similar charged-kaon excesses in earlier

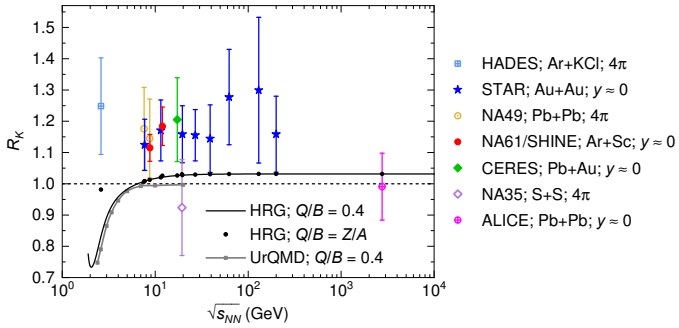

Fig. 7. Ratio of charged to neutral K meson yields in nucleus–nucleus collisions as a function of collision energy. Vertical bars denote total uncertainties. Figure from Ref. [19] with the new preliminary point at 8.8 GeV added.

nucleus–nucleus collision experiments. The Hadron Resonance Gas (HRG) model predictions for the ratio of net electric charge to net baryon number, $Q/B = 0.4$, are shown by the black line, with corresponding experimental Q/B values marked by black dots; gray squares denote UrQMD results. Neither model reproduces the experimental data. In 2024, NA61/SHINE performed measurements of K^0_S production in comparison with K^+ and K^- in $\pi^- + \mathrm{C}$ collisions at 158 and 350 GeV/c. As can be seen in Fig. 8, models fail to describe the ratio of charged to neutral kaons even for small asymmetric systems.

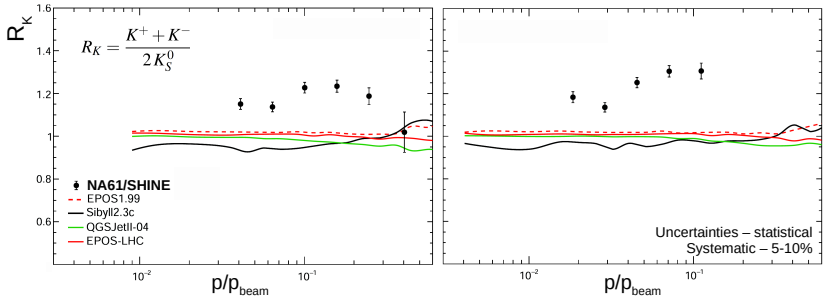

Fig. 8. Charged-to-neutral kaon ratio in $\pi^- + \mathrm{C}$ collisions at 158 (left) and 350 GeV/c (right) [20].

2.3. Future plans of NA61/SHINE

After the CERN Long Shutdown 3, NA61/SHINE plans continuation of 2D scan with B+B, O+O, and Mg+Mg collisions at $\sqrt{s_{NN}} = 5.1,\ 7.6$, and 16.8 GeV. The proposed measurements will enable a clear differentiation between the two limiting cases — light and heavy collision systems — and will substantially enhance our experimental understanding of the transition in the particle-production mechanism from light to medium-sized nuclei. More information on the hypothetical B+B, O+O, and Mg+Mg results can be found in Ref. [21]. The planned measurements will also allow for the study of isospin-symmetry violation in the isospin-symmetric systems ${}^{16}_{8}\mathrm{O} + {}^{16}_{8}\mathrm{O}$ and ${}^{24}_{12}\mathrm{Mg} + {}^{24}_{12}\mathrm{Mg}$. A pilot run with O+O at 16.8 GeV was recorded in 2025, and the data is currently being analyzed. In 2024, π^++C and π^-+C interactions at a beam momentum of 158 GeV/c were recorded. The new data will allow one to test whether $\pi^+ + \mathrm{C}$ interactions are the mirror image of $\pi^- + \mathrm{C}$ interactions with respect to $R_K = 1$, as expected from isospin symmetry.

REFERENCES

[1] NA61/SHINE Collaboration (N. Abrgall *et al.*), *J. Instrum.* **9**, P06005 (2014).

[2] M. Gaździcki, M.I. Gorenstein, *Acta Phys. Pol. B* **30**, 2705 (1999).

[3] NA49 Collaboration (C. Alt *et al.*), *Phys. Rev. C* **77**, 024903 (2008).

[4] K. Werner, *Nucl. Phys. B Proc. Suppl.* **175–176**, 81 (2008).

[5] J. Mohs, S. Ryu, H. Elfner, *J. Phys. G: Nucl. Part. Phys.* **47**, 065101 (2020).

[6] V. Kireyeu *et al.*, *Eur. Phys. J. A* **56**, 223 (2020).

[7] A. Motornenko *et al.*, *Phys. Rev. C* **99**, 034909 (2019).

[8] NA61/SHINE Collaboration (H. Adhikary *et al.*), *Eur. Phys. J. C* **84**, 416 (2024).

[9] NA61/SHINE Collaboration (A. Acharya *et al.*), *Eur. Phys. J. C* **81**, 73 (2021).

[10] NA61/SHINE Collaboration (A. Aduszkiewicz *et al.*), *Eur. Phys. J. C* **77**, 671 (2017).

[11] M. Stephanov, K. Rajagopal, E. Shuryak, *Phys. Rev. D* **60**, 114028 (1999).

[12] NA61/SHINE Collaboration (H. Adhikary *et al.*), *Eur. Phys. J. C* **84**, 741 (2024).

[13] NA61/SHINE Collaboration (H. Adhikary), *EPJ Web Conf.* **274**, 06008 (2022).

[14] NA61/SHINE Collaboration (V.Z. Reyna Ortiz), *Ukr. J. Phys.* **69**, 858 (2024).

[15] A. Bialas, M. Gazdzicki, *Phys. Lett. B* **252**, 483 (1990).

[16] NA61/SHINE Collaboration (H. Adhikary *et al.*), *Eur. Phys. J. C* **83**, 881 (2023).

[17] H. Rieger, *Phys. Rev. B* **52**, 6659 (1995).

[18] NA61/SHINE Collaboration (H. Adhikary *et al.*), *Eur. Phys. J. C* **83**, 919 (2023).

[19] NA61/SHINE Collaboration (F. Giacosa *et al.*), *Nat. Commun.* **16**, 2849 (2025).

[20] NA61/SHINE Collaboration (H. Adhikary *et al.*), *Phys. Rev. D* **107**, 062004 (2023).

[21] NA61/SHINE Collaboration (H. Adhikary *et al.*), Technical Report CERN-SPSC-2023-022; SPSC-P-330-ADD-14, CERN, 2023.